Nuclear structure of $^{146-154}$Sm in the dynamic pairing-plus-quadrupole model

J. B. Gupta
Ramjas College, University of Delhi, Delhi-7, India
(Received 28 February 1983)

The changes in the nuclear structure of $^{146-154}$Sm isotopes have been studied in the dynamic pairing-plus-quadrupole model. The overall variation in the energy of levels of g-, β-, and γ-vibrational bands; shape parameters; absolute $B(E2)$ values; $E0$ moments; and $E2$ branching ratios is given correctly. The effect of the change in the nature of the 2_2 (2_3) state at $N \leq 86$ on various transition moments is discussed. Increased asymmetry in lighter Sm isotopes is placed in the proper perspective. Comparison is made with other nuclear models.

[NUCLEAR STRUCTURE Dynamic pairing-plus-quadrupole model, $^{146-154}$Sm, calculated level energies, static moments, $B(E2)$ values, and $E0$ moments. Triaxiality.]

I. INTRODUCTION

The shape transitional region of rare earth elements continues to provide a challenge for nuclear theory. The Sm isotopes have been studied extensively experimentally[1-6] and theoretically.[7-11] The pairing-plus-quadrupole model was used to predict the equilibrium shapes of nuclei and to study the transitional region of W-Os-Pt isotopes.[12] Later Kumar studied the transition at $N=88-90$ in Sm but reported divergence of certain $B(E2)$ ratios in β-g and γ-g transitions in ^{150}Sm and noted the apparent breakdown of the PPQ model,[7] as is also cited in Refs. 4 and 8–11.

The interacting boson model (IBM) provides an alternative approach in terms of s and d bosons. Scholten *et al.*[8] studied the $^{146-156}$Sm isotopes in the IBM and simulated the transition from the SU(5) to SU(3) limits of SU(6) by using symmetry breaking terms. Tamura *et al.*[9] questioned the justification of the order-of-magnitude variation,[8] with even a change of sign, of the parameters ϵ, k, and k' of the IBA-1 for Sm isotopes. They applied the boson expansion model (BEM) for $^{150-154}$Sm and used sixth order expansion to improve the agreement of $B(E2)$ values with experiment.[9] Recently, Casten compared PPQ, BEM, and IBM results for Sm isotopes[10] and again noted the inconsistent results[7] of the PPQ for ^{150}Sm.

Since the dynamic PPQ model had succeeded well for transitional nuclei W-Os-Pt,[12,13] and the $B(E2)$ ratios for γ-g and β-g transitions in the $N=88$ isotone ^{152}Gd showed no such divergence,[14] we restudied ^{150}Sm in the DPPQ model and noted[15] a delicate balance between pairing and quadrupole forces of $H_{\rm PPQ}$ in ^{150}Sm. However, even the rigid asymmetric rotor model (ARM) values were recently cited[11] to be better than the DPPQ ones.[7] As the $B(E2)$ values for γ-g and β-g transitions in Sm show some systematic variations with the neutron number N, we extend our study to the $^{146-154}$Sm isotopes and test how far the DPPQ model succeeds in reproducing these variations.

In Sec. II we briefly discuss the DPPQ model and the input parameters of the calculation. The DPPQ results are presented in Sec. III and compared with other models. In Sec. IV we discuss the conclusions from this study.

II. THE DPPQ MODEL

In the dynamic pairing-plus-quadrupole model[13] used here, the seven parameters [$V(\beta,\gamma)$, $\mathcal{I}_k$, B_{k1}] of the collective Hamiltonian

$$H_c = V(\beta,\gamma) + \tfrac{1}{2}\sum_{k=1}^{3} \mathcal{I}_k(\beta,\gamma)\omega_k^2 + \tfrac{1}{2}B_{\beta\beta}(\beta,\gamma)\dot{\beta}^2 + \tfrac{1}{2}B_{\gamma\gamma}(\beta,\gamma)\beta^2\dot{\gamma}^2 + B_{\beta\gamma}\beta\dot{\beta}\dot{\gamma} \quad (1)$$

are derived from the time-dependent Hartree-Bogolyubov (TDHB) treatment of $H_{\rm PPQ}$. Limiting ourselves to small amplitude, quadrupole motion of the nucleus, a generalized rotational basis (GRB)

$$\psi_{\alpha IM} = \sum_K A_{\alpha IK}(\beta,\gamma)\phi^I_{MK}(\phi\theta\psi) \quad (2)$$

(ϕ's are the symmetrized sum of rotational matrices D^I_{MK}) is employed. The GRB is valid in both the rotational and vibrational limits of H_c, corresponding to SU(3) and SU(5) limits of the SU(6) group. Complete freedom in β, γ space is allowed not only for the potential $V(\beta,\gamma)$, but also for the moments of inertia $\mathcal{I}_k$ and the mass coefficients B_{k1}, so that the oblate, prolate, triaxial, and γ-unstable [=O(6) symmetry] shapes are allowed in a natural way.

Limiting ourselves to only $J=2$, $T=0$ types of p-h coherent admixtures and $J=0$, $T=1$ types of p-p and h-h pairs treated by quadrupole and pairing forces, respectively, a large configuration space of 36 single particle orbits for protons, and 49 for neutrons, each spread over two oscillator shells, is used. The $Z=40$, $N=70$ inert core contribution is taken into account through a core renormalization factor F_B for the mass coefficients (see Table I). Slight variation has been allowed also in the quadrupole force constant X_0. The nucleon effective charge e_n (e_p) was kept constant.

TABLE I. Parameters of the DPPQ model calculation for Sm isotopes.

Parameter	A 146	148	150	152	154
Quadrupole force X_0 in $X=X_0A^{-1.4}$	75.5	70	70	70	69
Inertial renormalization factor F_B	3.0	3.0	2.0	2.2	2.25
Effective charge e_n ($e_p=1+e_n$)			$1.65Z/A$		

III. RESULTS AND DISCUSSION

A. Potential energy surface parameters

The potential energy surface (PES) $V(\beta,\gamma)$ and its $V(\beta,\gamma=0)$ cuts for Sm isotopes (Fig. 1) exhibit the change in nuclear shape with N. The equilibrium deformation β_0 for $V=V_{\min}(\beta,\gamma=0)$ falls to zero at $N=86$, but $\beta_{\rm rms}\neq 0$ (Table II), even at $N=84$ in ^{146}Sm, which has a tendency towards prolate deformation [e.g., see the $V=2$ MeV curve in Fig. 1(a)], as does ^{148}Sm. Similarly, $\gamma_0=0$ for all N, but not $\gamma_{\rm rms}$, which increases to almost 30° for lighter isotopes. Symmetry of equipotential lines in the γ direction about $\beta_0=0$ in the (β,γ) plane causes γ softness and leads to large $\gamma_{\rm rms}$'s for lighter isotopes. This asymmetry is also reflected in the moments of inertia $\mathcal{I}_k$ at $\beta=\beta_{\min}$. While $\mathcal{I}_1\simeq\mathcal{I}_2$ (for $\mathcal{I}_3$ small) for deformed isotopes, $\mathcal{I}_1>\mathcal{I}_2\simeq\mathcal{I}_3$ (all $\mathcal{I}$'s being small) for light anharmonic vibrators (see Table II).

The values of γ_0 used[11] in the ARM for $^{150-154}$Sm derived from E_{2_γ}/E_{2_g} or $Q(2^+)_{\rm exp}$ are close to our $\gamma_{\rm rms}$ values, but these are not β-rigid asymmetric rotors at all, as assumed in ARM, and taking $\gamma_0=\gamma_{\rm rms}$ is rather a simplification. The asymmetry is not in the equilibrium shapes, but instead is due to γ vibration about small or zero β_0.

The energy of deformation ($E_{\rm def}$), the prolate-oblate difference $V_{\rm PO}$, and the zero point energy W_0 (Table II) also reflect the shape changes with neutron number N.

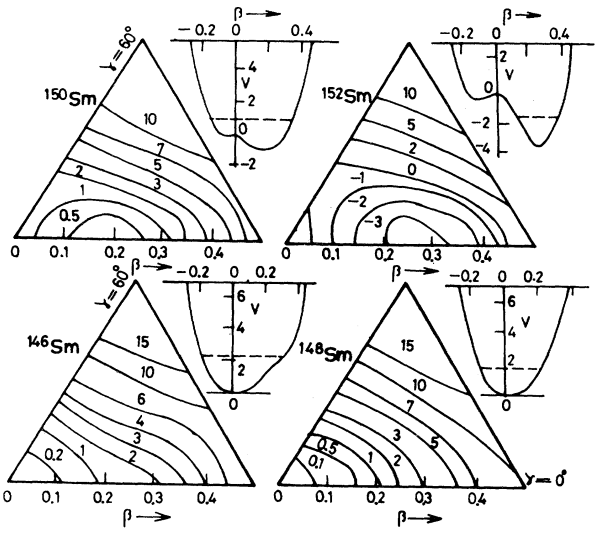

FIG. 1. $V(\beta,\gamma)$ in MeV for $^{146-152}$Sm isotopes in the $(\beta,0\leq\gamma\leq 60°)$ plane. The cuts $V(\beta,\gamma=0)$ are also given.

B. The level energies and K structure

The fast decrease of the energy of 2_1^+ and 4_1^+ states at $N=88-90$ representing a spherical-deformed shape change is reproduced here (Table III). Even at $N=84$, the second excited state is 4^+, followed by 0^+ and 2^+. This feature of the rotation model is also reproduced. On the other hand, the energy of the 0_2^+ β bandhead first falls with an increase in neutron number, is minimum at $N=88-90$, and then rises again. This variation is also given from theory, though not the full lowering at $N=88-90$.

The K-component structure [see Eq. (2)] for the lowest 2^+ states shows the increased band mixing for softer light isotopes, and a change in the nature of 2^+ states (Table IV). The 2_2 (2_3) state is β- (γ)-vibrational $K^\pi=0^+$ in $^{150-154}$Sm, but in ^{148}Sm the 2_2 state becomes predominant-

TABLE II. Potential energy surface parameters, and moments of inertia at $\beta=\beta_{\min}$.

Quantity	A 146	148	150	152	154
$\beta_{\min}$	0.0	0.0	0.205	0.236	0.267
$\beta_{\rm rms}$ (g.s.)	0.142	0.146	0.20	0.258	0.283
$\beta_{\rm rms}$ (2^+)	0.171	0.173	0.22	0.265	0.285
$\gamma_{\rm rms}$ (g.s.)	28°	26°	20°	15°	13°
$E_{\rm def}$[a] (MeV)	0	0	1.0	3.4	5.4
PO difference (MeV)	0	0	0.85	2.8	3.8
Zero point energy (MeV)	2.35	1.77	1.92	2.0	2.0
$\mathcal{I}_1$ at $V_{\min}$ (MeV^{-1})	0.97	1.9	23.1	40	44
$\mathcal{I}_2$	0.27	0.5	19	33	37
$\mathcal{I}_3$	0.24	0.44	0.32	0.44	0.43

[a]Values for $^{150-154}$Sm of $E_d=0.8$, 2.5, and 4.3 MeV obtained by Ragnarsson *et al.* (Ref. 27) using the improved Nilsson model are close to ours, as are also their values of 0.6, 1.4, and 2.6 MeV, respectively, for $V_{\rm PO}$.

TABLE III. The energy (keV) of low lying states of Sm isotopes.

State		A 146	148	150	152	154
2_1^+	exp[a]	0.747	0.550	0.334	0.122	0.082
	th	0.756	0.564	0.338	0.121	0.086
4_1^+	exp	1.381	1.180	0.773	0.366	0.267
	th	1.375	1.134	0.747	0.361	0.270
$0'$	exp	1.452	(1.120)	0.740	0.685	1.100
	th	1.430	1.242	1.049	1.00	1.096
2_2^+	exp	1.648	1.454	1.046	0.811	1.178
	th	1.725	1.487	1.460	1.211	1.198
2_3^+	exp	(2.156)	1.663	1.194	1.084	1.440
	th	2.310	2.13	1.782	1.556	1.537

[a]The energies are from a compilation in Ref. 16.

ly $K^\pi=2^+$, and 2_3 is $K^\pi=0^+$. This is in contrast to Ref. 8 but agrees with Ref. 16. The K structure is less relevant in ^{146}Sm. Although $K^\pi=0^+$ is 66% in 2_2, 2_3 is also $\sim 50\%$ $K^\pi=0^+$, consistent with Ref. 16.

The 4_2 (4_3) state is $K^\pi=0^+$ (2^+) in all five isotopes, with the largest mixing in ^{148}Sm. The nature of the fourth 4^+ state changes substantially with n^0 number. While it is 2β vibrational in ^{152,154}Sm, it is $K^\pi=2^+$ $\beta\gamma$ in ^{150}Sm and a $K^\pi=4^+$ 2γ state in ^{148}Sm, again reflecting a change from a β-soft to γ-soft nuclear core.

C. The deformation parameters

The quadrupole moment

$$Q(2^+)=\left[\frac{16\pi}{5}\right]^{1/2}\langle 2\,|\,M(E2)\,|\,2\rangle\ ,$$

which is a good measure of deformation, varies smoothly with n^0 number [see Fig. 2(a)], and is given correctly from the calculation. The gyromagnetic ratio $g_I=\mu_I/I$ is equal to Z/A in the rotational model. The small variation of $g(2^+)$ from Z/A is a measure of the relative density distribution of protons and neutrons. The $g(2^+)$ in Sm seems to increase as N increases. This is also indicated roughly in our calculation.

The isomer shift

$$(\mathrm{IS})=\delta\langle r^2\rangle/\langle v^2\rangle$$

between 0_1^+ and 2_1^+ states is indicated to be constant up to $N=88$ and falls at $N=90$ and 92, showing rigidity to centrifugal stretching in deformed nuclei. This trend agrees with experiment and IBA results, although numerically DPPQ values are almost twice, and IBA values half, of the experiment.

The monopole matrix element $\rho_{if}(E0)$ ($I_i=I_f$) is proportional to off-diagonal matrix elements of r^2. In the vibrational limit SU(5) $\rho(E0)=0$, but is allowed in the rotational limit SU(3), and increases as $n^{1/2}$ (n is the number of boson pairs).[8] Without normalization our results agree with the available data and reproduce the smooth increase with N for 0_2-0_1 and 2_2-2_1 transitions [Fig. 2(b)]. For (γ-g) 2_3-2_1 $E0$ is expected to be small, and predicted variation with N agrees with the IBA (Ref. 8) except in the position of maximum at $N=86$ in the DPPQ, which reflects the change to the β state in ^{148}Sm.

D. Absolute $B(E2)$ values

The Coulomb excitation and lifetime measurements provide accurate $B(E2)$ values of collective states at low energy. The sharp increase of $B(E2;2_1-0_1)$ and $B(E2;4_1-2_1)$ with increasing neutron number, reflecting increased deformation, is given correctly without varying

TABLE IV. The relative contribution (in %) of the $K^\pi=0^+$ component in 2^+ and 4^+ states of Sm. The $K^\pi=2^+$ percentage is given in parentheses. The balance is $K^\pi=4^+$.

State	A 146	148	150	152	154
2_1	91.1	93.7	99.2	99.9	99.96
2_2	66.3	40.4	65.4	98.0	99.5
2_3	50.0	55.7	37.0	3.1	0.6
4_1	89.4	93.3	98.9	99.7	99.9
	(8.4)	(5.8)	(1.0)	(0.3)	(0.1)
4_2	81.2	48.6	80.4	97.5	98.8
	(13.2)	(40.9)	(17.9)	(2.5)	(1.2)
4_3	42.7	41.0	23.4	5.0	1.7
	(49.3)	(57.8)	(73.0)	(94.4)	(98.1)
4_4	38.4	22.5	23.3	92.7	91.1
	(57.2)	(21.2)	(38.8)	(6.9)	(8.4)

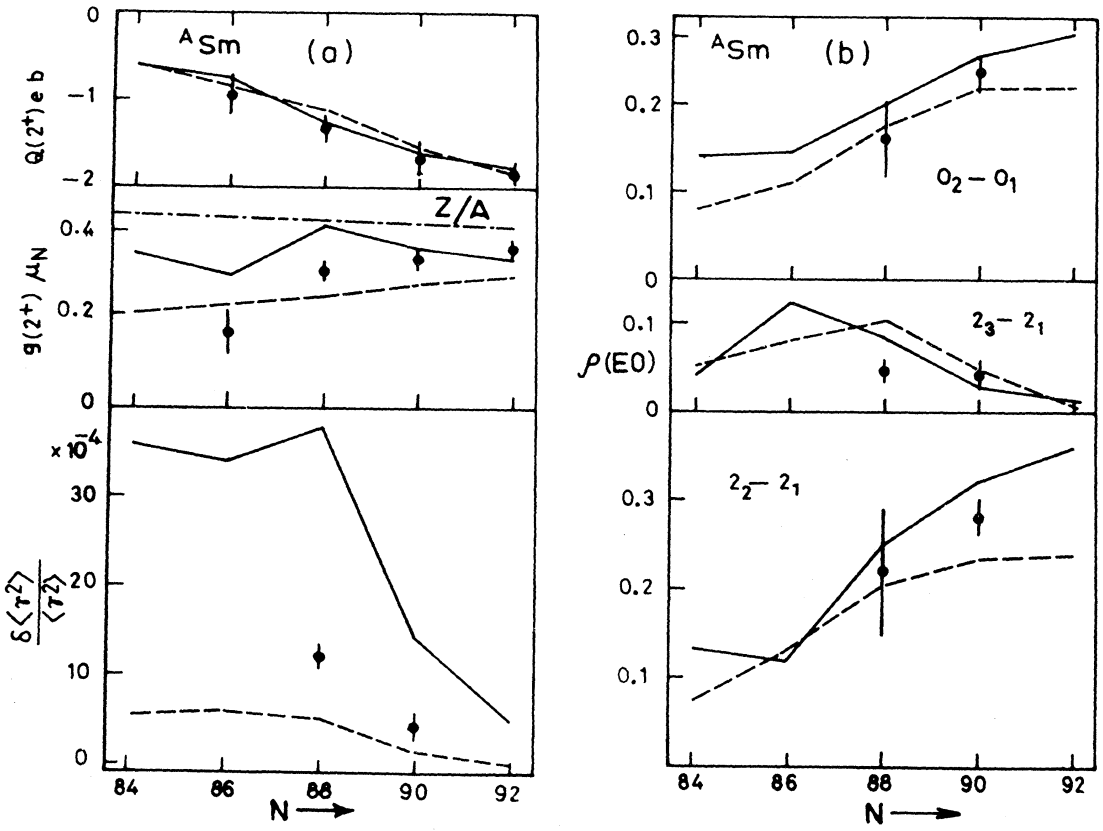

FIG. 2. (a) Calculated DPPQ values (full lines) are compared with IBM values (dashed lines) and experiment (data points). Quadrupole moments $Q(2^+)$, gyromagnetic ratio $g(2^+)$, and isomer shift data are from Refs. 17, 18, and 19, respectively. $Q(2^+,{}^{154}\mathrm{Sm})$ is deduced from $B(E2,0\text{-}2)$; $g(2^+)$ values are weighted averages (Ref. 18). (b) Data points are from Ref. 20.

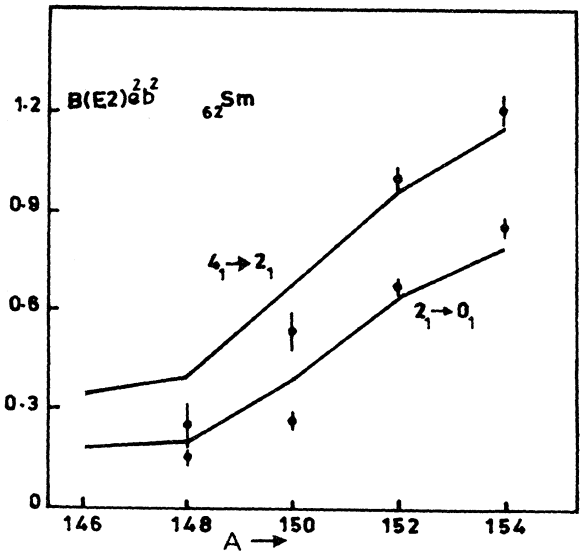

FIG. 3. Comparison between calculated (full line) and experimental (points) (Refs. 21 and 22) $B(E2)$ values in the Sm isotopes.

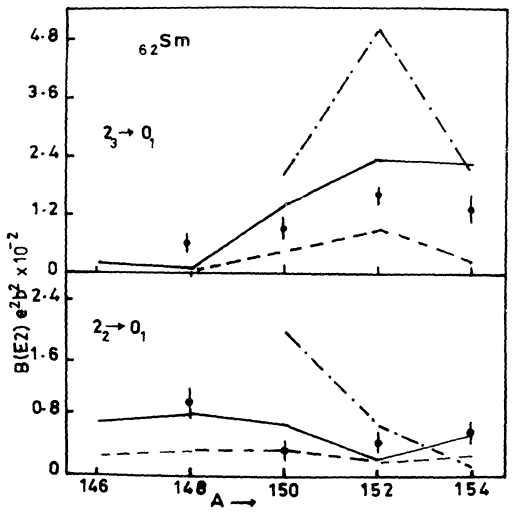

FIG. 4. Absolute $B(E2)$ values for 2_2^+-0_1^+ and 2_3^+-0_1^+ transitions in Sm isotopes. The data points are taken from Refs. 9 and 22. The full line represents DPPQ values, the broken line the IBM (Ref. 8), and the dashed-dotted line the TWK (Ref. 9) BEM values.

TABLE V. Absolute $B(E2)$ values (e^2b^2) for 2_2 and 4_2 states to g-band transitions in Sm isotopes.

				A		
I'	I_g	146	148	150	152	154
0_2	2_1	exp[a]		0.26 (3)	0.176(11)	
		th 0.34	0.38	0.43	0.166	0.094
		BEM		0.42	0.120	0.054
2_2	0_1	exp	0.010(2)[c]	0.004(2)	0.0046(3)	0.0060(14)
		th 0.0073	0.009	0.0074	0.0022	0.0055
		BEM		0.020	0.007	0.001
2_2	2_1	exp	0.16(4)[c]	0.043(20)	0.026(3)	0.012
				0.27(15)[b]		
		th 0.143	0.192	0.108	0.029	0.021
		BEM		0.181	0.025	0.010
2_2	4_1	exp		0.17(10)	0.091(11)	0.024
				0.55(30)[b]		
		th 0.083	0.074	0.10	0.089	0.062
		BEM		0.077	0.07	0.008
4_2	2_1	exp			0.0053(35)	
		th 0.0017	0.006	0.00035	0.0006	0.003
		BEM		0.007	0.005	0.018
4_2	4_1	exp			0.037(23)	
		th 0.078	0.123	0.063	0.026	0.020
		BEM		0.105	0.016	0.003

[a]Experimental values are taken from Ref. 9.
[b]Reference 4.
[c]Reference 22.

the effective charge of the nucleons (see Fig. 3).

The $B(E2;2_2\text{-}0_1)$ value decreases slowly with neutron number up to $N=90$, but is enhanced in ^{148}Sm. (Note the effect of the change of the nature of the 2_2 state to γ vibration.) While the IBM values[8] are generally smaller and the BEM values[9] diverge at $N=88$, the DPPQ values give the required variation (see Fig. 4).

The $B(E2;2_3\text{-}0_1)$ value shows a maximum at $N=90$ in ^{152}Sm (see Fig. 4). In ^{154}Sm, the value is smaller due to less β-g mixing, while in ^{148}Sm the natures of the 2_2 and 2_3 states interchange (see Sec. III B). The DPPQ values vary as in experiment, while BEM again diverges at $N=90$. IBM values are somewhat smaller. Note that in the IBM a β_2' parameter of the symmetry breaking term was used for obtaining the small $B(E2;2_3\text{-}0_1)$ values,[8] while no fitting is resorted to in the present approach. Also note the factor of 100 variation between $2_1\text{-}0_1$ and $2_2(2_3)\text{-}0_1$ $B(E2)$ values reproduced here. Further comparison of $B(E2)$ values for other β-g and γ-g transitions is made in Tables V and VI. There is a fair overall agreement of the theoretical values.

E. Reduced interband $B(E2)$ ratios

Interband $B(E2)$ ratios are sensitive to band mixing effects, deviating widely from rotation model values, and thus provide stringent tests of the wave functions and their relative phases and also of $E2$ operators used in the model.

TABLE VI. Absolute $B(E2)$ values (e^2b^2) for 2_3 and 4_3 states to g-band transitions in Sm isotopes.

				A		
I'	I_g	146	148	150	152	154
2	0	exp[a]	0.006[b]	0.009(2)	0.016(1)	0.013(3)
		th 0.0009	0.00045	0.014	0.023	0.022
2	2	exp		0.039(14)	0.042(4)	0.02
		th 0.059	0.010	0.027	0.048	0.039
		BEM		0.024	0.053	0.047
2	4	exp		0.019(10)	0.004(3)	0.0008
		th 0.023	0.110	0.054	0.006	0.0046
		BEM		0.087	0.006	10^{-5}
4	2	exp			0.0035(1)	
		th 0.0005	3×10^{-6}	0.009	0.009	0.0093
		BEM		0.022	0.026	0.021
4	4	exp			0.037(1)	
		th 0.057	0.010	0.035	0.047	0.043
		BEM		0.032	0.076	0.040

[a]The experimental data values are taken from Ref. 9.
[b]Reference 22.

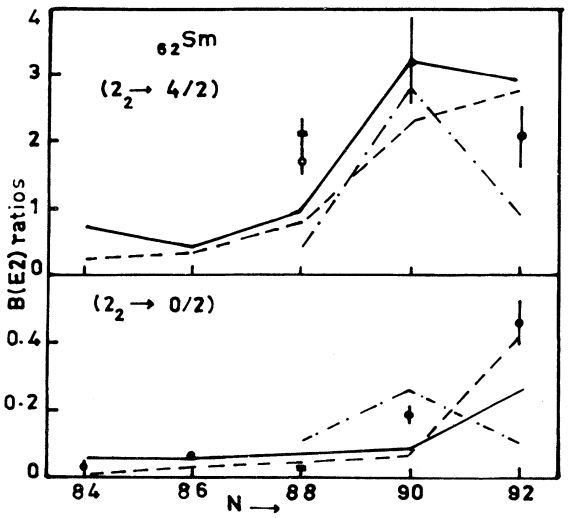

FIG. 5. $B(E2)$ ratios for 2_2 g-band transitions. Filled circle data points are calculated values using branching ratios (Ref. 23), unfilled circles are from Ref. 8, and squares are from Ref. 4. Also see the caption to Fig. 4.

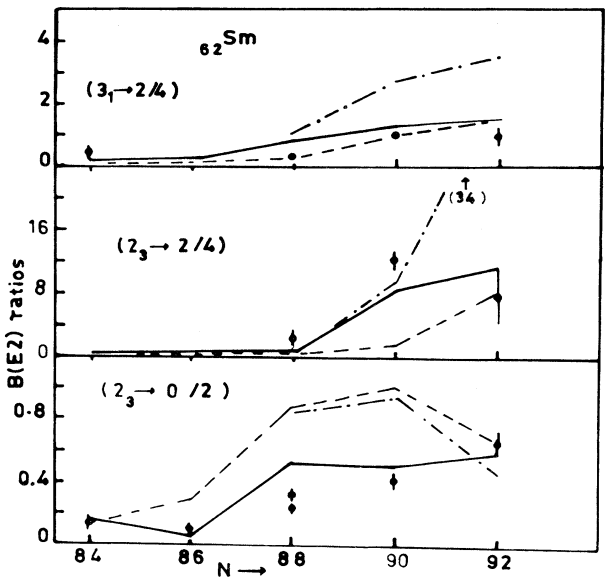

FIG. 6. $B(E2)$ ratios for 2_3 and 3_1 g-band transitions. See the captions to Figs. 4 and 5.

The variations in the $B(E2)$ ratios for β-g and γ-g transitions with neutron number are given correctly in the present calculation. The order of magnitude deviation observed previously[4,7–11] for $B(E2;2_2\text{-}0_1/2_1)$ and $B(E2;2_2\text{-}4_1/2_1)$ ratios for $N=88$ is now removed, and the decreasing values right up to $N=84$ are reproduced (see Fig. 5). Note the wrong maximum in $B(E2;2_2\text{-}0_1/2_1)$ of the boson expansion model calculation.[9] Similarly the variations in the $B(E2;2_3\text{-}0_1/2_1)$, $B(E2;2_3\text{-}2_1/4_1)$, and $B(E2;3_1\text{-}2_1/4_1)$ with neutron number are reproduced closest in the DPPQ model in comparison to the BEM or the IBM (see Fig. 6).

Calculated $B(E2)$ ratios for several other β-g, γ-g transitions are presented in Tables VII and VIII. The decreasing or increasing trends of individual ratios with n^0 number are in most cases best reproduced in the DPPQ compared to the BEM or IBM. The maximum deviations occur for those ratios in which one or both transitions are weak. Slight variation of input parameters (X_0 or F_B) produces a large increase or decrease (by a factor of 10^2 or more) in these cases, especially in softly deformed nuclei.

IV. CONCLUSIONS

The validity of the dynamic pairing-plus-quadrupole model[13] is tested for the full range of Sm isotopes with a single set of parameters, except the X_0 and F_B factors, which were varied slightly (see Table I). The large value

TABLE VII. The $B(E2)$ ratios for β-g transitions in Sm.

			A				
I_i	$I_f/I_{f'}$		146	148	150	152	154
2_2	$0'/0$	exp[a]			181(56)		
					28(4)[b]	<4300[c]	
		PPQ	30	150	41	291	159
		BEM			9.5	69	616
4_2	2/4	exp	<0.25(5)[d]	>0.03(1)	0.0024(5)[b]	0.13(5)[e]	0.9(5)
		PPQ	0.02	0.05	0.0056	0.023	0.16
		BEM			0.056	0.32	6.48
4_2	$2_2/4$	exp			5.9(9)[b]	45(3)[c]	
		PPQ	5.4	2.5	9.1	43	66
		BEM			3.36	39	318
4_2	$2_2/3$	exp			2470(850)[b]	350(170)	
		PPQ	256	51	1622	1831	415
		BEM			60	123	49

[a]Experimental values deduced using branching ratios from Table of Isotopes (Ref. 23), assuming pure $E2$.
[b]Reference 9.
[c]Konijn *et al.* (Ref. 24).
[d]Large $M1$ is indicated in the 4_2-2_1 transition (Ref. 23).
[e]Corrected for 16% $M1$.

TABLE VIII. The $B(E2)$ ratios for 2_3, 3_1, and 4_3 states to g-band transitions in Sm isotopes.

I_i	$I_f/I_{f'}$		A 146	148	150	152	154
2_3	$0'/0$	exp[a]			4.1(10)		
		PPQ	77	371	6.4	0.024	0.001
		BEM			4.9	0.42	0.80
	$2_2/2$	exp			12(6)[b]	1.2(1)	
		PPQ	3.6	22	19	2.50	1.11
		BEM			12	2.64	0.70
3_1	$2_3/2$	exp			17(6)		
		PPQ	22	16	13	25	33
		BEM			4.34	8.9	34
	$2_2/2$	exp	$>5.5(28)$		3.6(14)	≤ 0.06	
		PPQ	10	15	3.5	0.026	0.003
		BEM			1.8	0.40	0.63
4_3	2/4	exp		$<0.10(2)$	0.060(7)	0.10(5)	0.055[b]
		PPQ	0.1009	0.0003	0.26	0.18	0.22
		BEM			0.69	0.34	0.51
	$2_2/2$	exp			$<2.95(59)$[b,c]	0.8(4)	
		PPQ	5.3	10^3	0.02	0.2	0.18
		BEM			0.08	1.65	2.77

[a]See note for Table VII.
[b]Reference 9.
[c]Only an upper limit for $I_\gamma(4_3\text{-}2_2)$ is given (Ref. 23) (also see text).

of 3—5 for the core renormalization factor F_B used previously[7] is now reduced to only 2—3. Furthermore, it is interesting to observe that the value of the quadrupole force parameter X_0 is critical only for the $N=88$ isotopes of Sm and Nd (Ref. 25), reflecting the softness of these nuclei to shape deformation, but is not critical for the isotone ^{152}Gd. This is clearly a shell effect and provides independent evidence for a $Z=64$ magic number.[26]

The calculated values of the PES parameters (β_0, γ_0; $\beta_{\rm rms}$, $\gamma_{\rm rms}$; $E_{\rm def}$, $V_{\rm PO}$, W_0) and $Q(2^+)$, $g(2^+)$, isomer shift, $\rho(E0)$, and energy values present a coherent and varied picture of the changes in nuclear equilibrium shapes and nuclear dynamics with n^0 number in Sm isotopes. The observed maxima/minima or monotonic variations with N of the absolute $B(E2)$ values and $B(E2)$ ratios are also fairly well reproduced.

The use of (β_0,γ_0) and $(\beta_{\rm rms},\gamma_{\rm rms})$ in distinguishing between the β-rigid triaxial and γ-soft vibration is illustrated here; it can be of general utility. Thus we have illustrated the $P+Q$ residual interaction to be a good approximation when the average nuclear potential is also treated properly as was done here, and the time-dependent HB technique is utilized in treating the pairing and quadrupole forces adequately. A wide range of nuclear structure characteristics can be predicted without the need of a detailed fit to experimental data in individual nuclei.

ACKNOWLEDGMENTS

I am indebted to Professor K. Kumar at Cookeville, Tennessee, for useful discussions and to Dr. G. P. Srivastava, Chairman, Physics Department of the University of Delhi, for providing the facility for this study and for encouragement. The work was supported in part by the University Grants Commission of India.

[1]K. R. Baker, J. H. Hamilton, and A. V. Ramayya, Z. Phys. A 256, 387 (1972).
[2]H. Yamamoto, K. Kawade, E. Fukaya, and T. Katoh, J. Phys. Soc. Jpn. 37, 10 (1974).
[3]C. A. Kalfas, J. Phys. G 3, 929 (1977).
[4]M. Hoshi and Y. Yoshizawa, J. Phys. Soc. Jpn. 42, 1106 (1977).
[5]B. Harmatz and J. R. Shepard, Nucl. Data Sheets 20, 373 (1977); 26, 281 (1979).
[6]C. M. Baglin, Nucl. Data Sheets 18, 223 (1976); 30, 1 (1980).
[7]K. Kumar, Nucl. Phys. A231, 189 (1974).
[8]O. Scholten, F. Iachello, and A. Arima, Ann. Phys. (N.Y.) 115, 325 (1978).
[9]T. Tamura, K. Weeks, and T. Kishimoto, Phys. Rev. C 20, 307 (1979).
[10]R. F. Casten, Nucl. Phys. A347, 173 (1980).
[11]K. K. Gupta, Y. P. Varshney, and D. K. Gupta, Phys. Rev. C 26, 685 (1982).
[12]K. Kumar and M. Baranger, Nucl. Phys. A110, 529 (1968); A122, 273 (1968), and earlier references.
[13]K. Kumar, *The Electromagnetic Interactions in Nuclear Spectroscopy*, edited by W. D. Hamilton (North-Holland, Amsterdam, 1975), p. 155.
[14]J. B. Gupta and K. Kumar, Nucl. Phys. and Solid State Phys. (India) 20B, 15 (1977).
[15]J. B. Gupta and K. Kumar, J. Phys. G 7, 673 (1981); Nucl. Phys. and Solid State Phys. (India) 21B, 19 (1978).
[16]M. Sakai and A. C. Rester, At. Data Nuclear Data Tables 20, 441 (1977).
[17]N. R. Johnson, M. W. Guidry, R. S. Sturm, E. Eichler, R. O. Sayer, D. C. Hensley, and N. C. Singhal, Phys. Rev. C 22, 2416 (1980); and see Refs. 5 and 6.
[18]H. W. Kugel, R. R. Borchers, and R. Kalish, Nucl. Phys. A186, 513 (1972); and see Ref. 6.
[19]G. M. Kalvius and G. K. Shenoy, Nucl. Data Tables 14, 639 (1974); Y. Yamazaki, E. B. Shera, M. V. Hoehn, and R. M.

Steffens, Phys. Rev. C 18, 1474 (1978); C. S. Wu and L. Wilets, Annu. Rev. Nucl. Sci. 19, 527 (1969); also see the second listing of Ref. 17.

[20]A. V. Alduschenkov and N. N. Voinova, Nucl. Data Tables 11, 299 (1972); J. Lange, K. Kumar, and J. H. Hamilton, Rev. Mod. Phys. 54, 119 (1982).

[21]R. M. Diamond, F. S. Stephens, N. Nakai, and R. Nordhagen, Phys. Rev. C 3, 344 (1971).

[22]E. Veje, B. Elbek, B. Herskind, and M. C. Oslesen, Nucl. Phys. A109, 489 (1968); W. Andrejtscheff, K. D. Shilling, and P. Manfrass, At. Data Nucl. Data Tables 16, 515 (1975).

[23]*Table of Isotopes*, 7th ed., edited by C. M. Lederer and V. S. Shirley (Wiley, New York, 1978).

[24]Jan Konijn *et al.*, Nucl. Phys. A373, 397 (1982).

[25]J. B. Gupta, in *Proceedings of the International Conference on Band Structure and Nuclear Dynamics, New Orleans,* edited by A. L. Goodman (North-Holland, Amsterdam, 1980), Vol. I, p. 66.

[26]K. S. Toth, Phys. Rev. C 22, 1341 (1980).

[27]I. Ragnarsson, A. Sobiczewski, R. K. Sheline, S. E. Larsson, and B. Nerlo-Pomorska, Nucl. Phys. A233, 329 (1974).